

Bearing Capacity of a Group of Stone Columns in Soft Soil

M. Etezzad¹; A. M. Hanna, F.ASCE²; and T. Ayadat³

Abstract: Installation of stone column is a viable, cost effective, and environmentally friendly ground-improvement technique. Columns are made of compacted aggregate and are installed in weak soil as reinforcements to increase the shear resistance of the soil mass and, accordingly, its bearing capacity. While a single stone column mostly fails by bulging, a group of stone columns together with the surrounding soil may fail by general, local, or punching shear mechanism, depending on the soil/columns/geometry of the system. The mode of failure of the reinforced ground could be identified based on the ground geometry and strength parameters of both stone column and soft soil. This paper presents an analytical model to predict the bearing capacity of soft soil reinforced with stone columns under rigid raft foundation subject to general shear-failure mechanism. The model utilizes limit-equilibrium method and the concept of composite properties of reinforced soil. The proposed theory was validated for the case of bearing capacity of footings on homogenous soil and via the laboratory and numerical results available in the literature for this case. Design procedure and charts are presented for practicing purposes. DOI: 10.1061/(ASCE)GM.1943-5622.0000393. © 2014 American Society of Civil Engineers.

Author keywords: Stone columns; Ground improvement; Bearing capacity; General shear failure; Limit equilibrium; Analytical model; Design theory; Geotechnical engineering.

Introduction

Stone columns generally are used as a soil-improvement technique to increase the bearing capacity and to reduce settlement of foundations on cohesive soft soil, to reduce liquefaction potential of cohesionless material under seismic loading, and to stabilize natural slopes and embankments. Furthermore, installation of the stone columns provides a shorter drainage pathway for the native soil resulting in an increase in the rate of consolidation and, accordingly, an acceleration of the settlement. Reviews of available works on modeling, testing, and analysis of soft soils reinforced with stone column were reported by McCabe et al. (2009), Mokhtari and Kalantari (2012), and Najjar (2013). McCabe et al. (2009) stated that the behavior of stone columns has yet to be captured fully by analytical and numerical techniques.

Hughes and Withers (1974) and Balaam and Booker (1981) utilized the concept of unit cell to predict the capacity of single stone column, which assumes that each column in the group has a tributary domain of the surrounding soil. The domain has a cylindrical shape with a rigid exterior wall and, therefore, there is no shear stress or lateral deformation on the outside boundaries of the cell (i.e., no interaction between columns within the group). The bulging failure mechanism was adopted to predict the capacity of a single column; then the capacity of a group of stone columns was taken as the total capacities of the individual columns in the group.

Madhav and Vitkar (1978) developed a theoretical model to predict the bearing capacity of single stone column or a granular trench using the upper-bound limit method of analysis and the general shear-failure mechanism. Based on the results of an experimental investigation, Barksdale and Bachus (1983) proposed an approximate approach, utilizing the undrained shear strength of the surrounding soil to predict the bearing capacity of the system. Priebe (1995) was the first to introduce the general shear-failure pattern and the equivalent width of foundation to predict the group capacity using the angle of shearing resistance of unreinforced ground and an averaged value of the cohesion of the assumed equivalent foundation width. Bouassida et al. (1995) developed a lower-bound solution of the composite cell model to estimate the capacity of a group of stone columns. Priebe (1995) developed a method to estimate the amount of settlement for end-bearing stone columns. Priebe (2005) proposed a similar method for floating stone columns. Ellouze et al. (2010) criticized the Priebe method for being inferior to other simple design methods for analyzing stone-column foundations.

Lee and Pande (1998) introduced the homogenization method, which assumes that the granular material of the column is scattered uniformly throughout the soil mass. They used finite-element technique for the composite material to predict the bearing capacity and settlement of the system.

Hu (1995) conducted experimental investigation on the capacity of a group of stone columns. He reported that bulging failure pattern suggested by Hughes and Withers (1974) was not observed during testing owing to the columns interaction within the group during loading. Furthermore, he concluded that shear-failure mechanism of the combined columns/soil system was the collapse pattern for the reinforced soil mass. Wehr (1999) and Muir Wood et al. (2000) investigated the performance of groups of stone columns using finite-element analysis. They confirmed the group interaction reported by Hu (1995). Using homogenization technique and applying finite-element technique, Lee and Pande (1998) reported that their numerical model compared well with the laboratory study conducted by Hu (1995). Investigations by McKelvey et al. (2004) showed that punching failure was more pronounced in the case of shorter stone columns. Numerical modeling conducted by Shahu

¹Geotechnical Engineer, Golder Associates, 6925 Century Ave., Suite 100, Mississauga, ON, Canada L5N 7K2.

²Professor, Dept. of Building, Civil and Environmental Engineering, Concordia Univ., Montreal, QC, Canada H3G 1M8 (corresponding author). E-mail: hanna@civil.concordia.ca

³Associate Professor, Dept. of Civil Engineering, Prince Mohammad Bin Fahd Univ., Khobar 34754, Saudi Arabia.

Note. This manuscript was submitted on September 20, 2012; approved on February 18, 2014; published online on February 20, 2014. Discussion period open until September 10, 2014; separate discussions must be submitted for individual papers. This paper is part of the *International Journal of Geomechanics*, © ASCE, ISSN 1532-3641/04014043(15)/\$25.00.

and Reddy (2011) on ground reinforced by stone columns confirmed Hu's observation with respect to the failure mechanism.

Bouassida et al. (2009) presented a model to estimate the bearing capacity of foundations reinforced by floating columns. Kaliakin et al. (2012) conducted a numerical model to study the behavior of geosynthetic encased stone columns in soft soil. They examined the shortcomings of different constitutive models, and emphasized the need of constitutive models that could capture accurately the volume change that occurs within the granular soil. Utilizing numerical simulation, Asgari et al. (2013) investigated the efficiency of stone columns to improve liquefiable soil layer. They concluded that the stone-column technique is an effective ground-improvement method to reduce the lateral deformation in a sand stratum due to seismic activity.

Hanna et al. (2013) presented a numerical model to examine the interaction of a group of stone columns. They reported that bulging failure of individual stone columns was not observed for soil having the area replacement ratio higher than 10%. Furthermore, the combined column/soil system failed in general, local, or punching shear-failure modes, depending on the geometry of the system and the soil characteristics. They reported that general shear failure was observed at higher area replacement ratios, which implies a reduction in column spacing and higher column diameter/foundation width ratio; otherwise local or punching shear failure may take place. They presented charts to identify the mode of failure for a given column/soil/geometry condition. Hu et al. (1997) reported no significant ground improvement for the area-replacement ratio of less than 10%. Furthermore, an area-replacement ratio greater than 35% is difficult to achieve owing to technology limitations. Stuedlein and Holtz (2013) reported that none of the analytical methods available in the literature are entirely satisfactory for a wide range of conditions. Also, Stuedlein and Holtz (2014) observed a similar trend for the estimation of the settlement of ground reinforced by stone columns, based on available theoretical methods.

Analytical Model

Fig. 1 presents the modes of failure that may take place in ground reinforced with stone columns, namely, general, local, or punching shear failure. As reported by Hanna et al. (2013), the mode of failure depends on the soil/column/geometry conditions.

In general shear failure, the surrounding soil moves horizontally and vertically beyond the reinforced area, making the columns bulge (only in the center columns) and buckle (in the exterior columns).

In developing the analytical model, the failure mechanism for a group of stone columns subjected to general shear failure was idealized in the present investigation in three zones as follows (Fig. 2):

1. Zone 1 is made of a wedge shape (block ABC), located immediately under the foundation and making an angle ψ with the horizontal axis (i.e., the soil surface). Following the classic theories for bearing capacity of shallow foundation, it is assumed that the wedge ABC moves together with the footing during loading.
2. Zone 2 consists of two log-spiral sections (curves CD and CF), which are originated at the lower point of the wedge (i.e., point C in Fig. 2). Owing to the discontinuity of the materials at the boundaries between the composite system and the soft soil, divergence of the log-spiral curves was noted. Consequently, each log-spiral section is made of two parts: one part is within the composite soil and the other part is in the surrounding soft soil.
3. Zone 3 is known as the passive Rankine section, where the failure surfaces are made of planes (DE and FG). This zone connects the log-spiral part to the ground surface.

Because of symmetry, only half of the failure mechanism was analyzed; equilibrium equations were written for each section; and

the passive forces due to the unit weight, cohesion, and surcharge pressure were considered separately.

Referring to Fig. 3, the sum of moments around point O_1 is

$$\begin{aligned} \Sigma M_{O_1} = 0 &\Rightarrow W_1 l_1 + W_2 l_2 + P_\gamma \left[\cos(\psi - \varphi_{\text{comp}}) \frac{B}{3} \right. \\ &\quad \left. + \sin(\psi - \varphi_{\text{comp}}) \left(\frac{B}{3} \tan \psi - y_1 \right) \right] \\ &= F \cos \delta (a \cdot AH - y_1) \end{aligned} \quad (1)$$

where W_1 = weight of material in the log-spiral block O_1CH given by

$$W_1 = \gamma_{\text{comp}} \frac{r_1^2 - r_0^2}{4 \tan \varphi_{\text{comp}}} \quad (2)$$

In Fig. 3, the lines O_1C and O_1H are arcs of the log-spiral defined as r_0 and r_1 , respectively. From the geometry, r_0 and r_1 were calculated as

$$r_0 = \frac{B}{2 \sin \theta_1} \quad (3)$$

and

$$r_1 = \frac{B}{2 \sin \theta_1} e^{\theta_1 \tan \varphi_{\text{comp}}} \quad (4)$$

Substituting Eqs. (3) and (4) into Eq. (2), the following equation can be written:

$$W_1 = \gamma_{\text{comp}} \frac{B^2 (e^{2\theta_1 \tan \varphi_{\text{comp}}} - 1)}{16 \sin^2 \theta_1 \tan \varphi_{\text{comp}}} \quad (5)$$

Furthermore, the weight of the triangle ACO_1 is given by

$$W_2 = \frac{1}{2} \gamma_{\text{comp}} \frac{B}{2} y_1 \quad (6)$$

where

$$y_1 = \frac{B(\tan \psi - \cot \theta_1)}{2} \quad (7)$$

Substituting Eq. (7) into Eq. (6) gives

$$W_2 = \gamma_{\text{comp}} \frac{B^2 (\tan \psi - \cot \theta_1)}{8} \quad (8)$$

The lever arm l_1 and l_2 are calculated as (Hijab 1956)

$$\begin{aligned} l_1 &= \frac{2B \tan \varphi_{\text{comp}}}{3 \sin \theta_1 (9 \tan^2 \varphi_{\text{comp}} + 1) (e^{2\theta_1 \tan \varphi_{\text{comp}}} - 1)} \\ &\quad \times \left[e^{3\theta_1 \tan \varphi_{\text{comp}}} - (3 \tan \varphi_{\text{comp}} \sin \theta_1 + \cos \theta_1) \right] \end{aligned} \quad (9)$$

$$l_2 = \frac{B}{6} \quad (10)$$

The height AH is

$$AH = H_1 = \frac{B}{2 \sin \theta_1} (\tan \psi \sin \theta_1 - \cos \theta_1 + e^{\theta_1 \tan \varphi_{\text{comp}}}) \quad (11)$$

Substituting Eq. (5) and Eqs. (7)–(11) into Eq. (1) gives

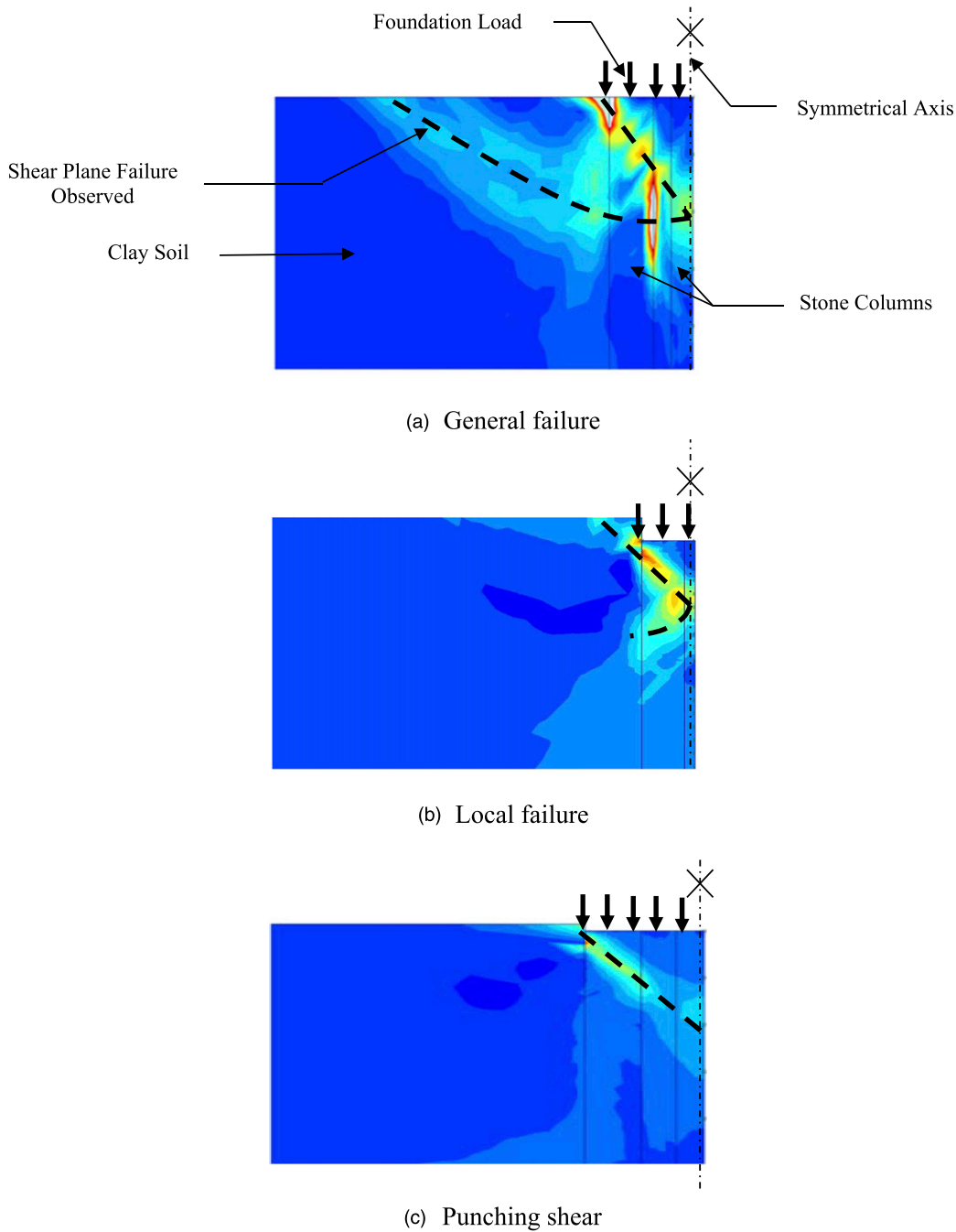


Fig. 1. Failure mechanisms of a group of stone columns in soft soil (Adapted from Hanna et al. 2013, © ASCE)

$$\gamma_{\text{comp}} \frac{B^3}{24 \sin^3 \theta_1 (9 \tan^2 \varphi_{\text{comp}} + 1)} \left[e^{3\theta_1 \tan \varphi_{\text{comp}}} - (3 \tan \varphi_{\text{comp}} \sin \theta_1 + \cos \theta_1) \right] + \gamma_{\text{comp}} \frac{B^3 (\tan \psi - \cot \theta_1)}{48} + P_\gamma \left\{ \cos(\psi - \varphi_{\text{comp}}) \frac{B}{3} + \sin(\psi - \varphi_{\text{comp}}) \left[\frac{B}{3} \tan \psi - \frac{B(\tan \psi - \cot \theta_1)}{2} \right] \right\} = F \cos \delta \left[a \cdot H_1 - \frac{B}{2} (\tan \psi - \cot \theta_1) \right] \quad (12)$$

It can be noted that the ultimate bearing capacity of the foundation system reaches a minimum value when the resistance force F is at its optimum value (i.e., $\partial F / \partial v = 0$), where v is a value related to the angle θ_1 (Kumbhojkar 1993).

By differentiating Eq. (12) with respect to θ_1 and equating the result to zero, the critical value of θ_1 and F can be estimated.

For the soft-soil section, by taking moments of all forces around point O_2 gives (Fig. 4)

$$\Sigma M_{O_2} = 0 \rightarrow \frac{q_1 \cos \varphi_c}{2} AD \left(\frac{2}{3} AD - AO_2 \right) + W_3 l_3 = W_4 l_4 + F \sin \delta \cdot x_2 + F \cos \delta (a \cdot AH - y_2) \quad (13)$$

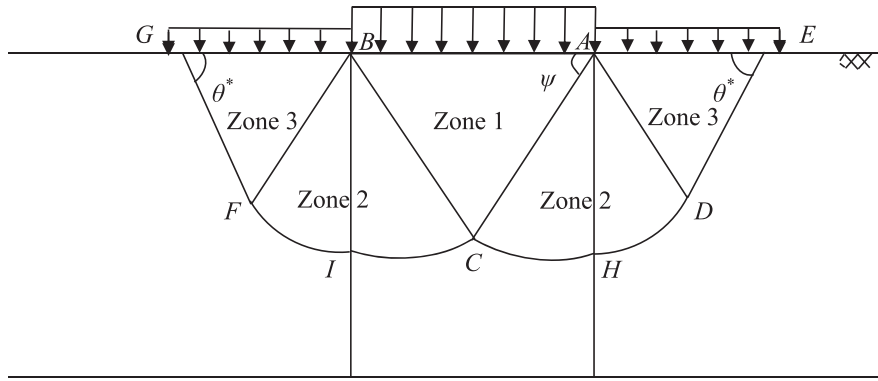


Fig. 2. Idealized failure mechanism

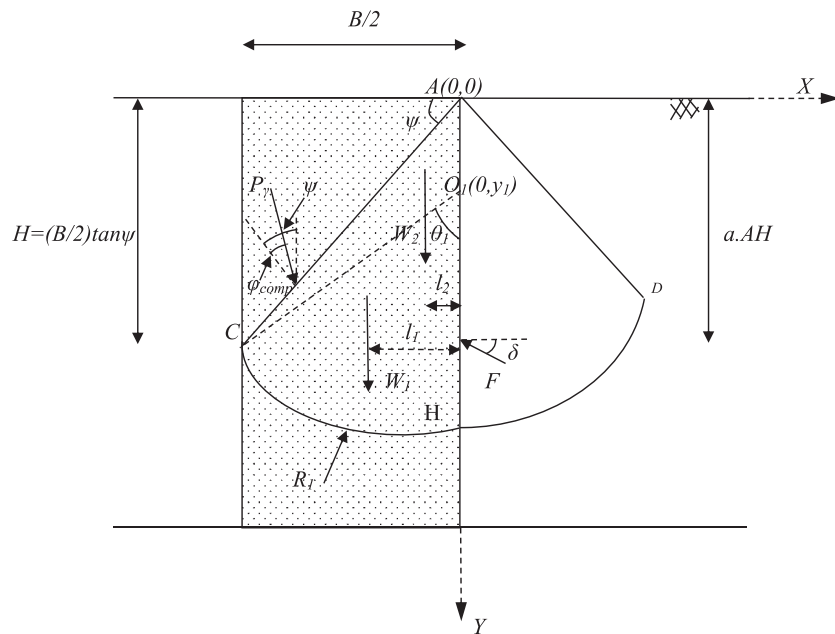


Fig. 3. Forces acting on the composite-soil section (case of: $\phi \neq 0, \gamma \neq 0, q = 0, c = 0$)

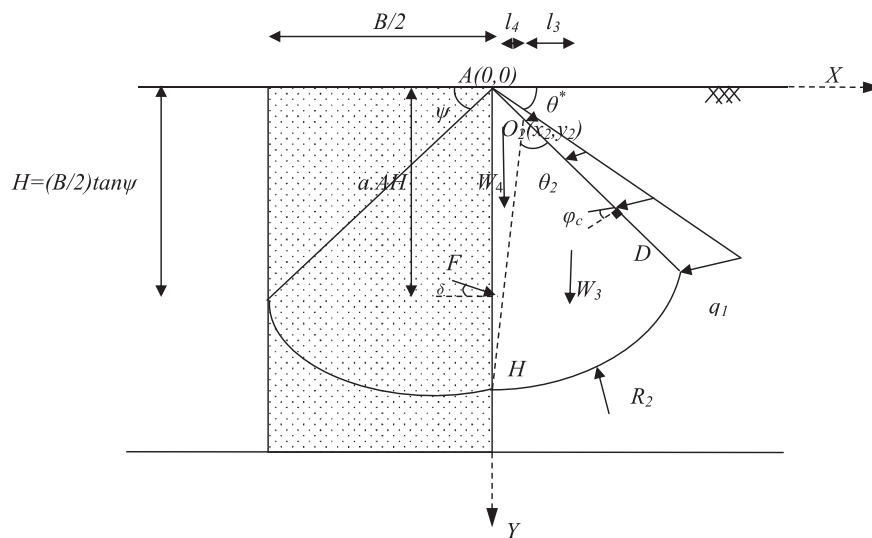


Fig. 4. Forces acting on the soft-soil section (case of: $\phi \neq 0, \gamma \neq 0, q = 0, c = 0$)

where W_3 = weight of the material in the log-spiral block O_2HD

$$W_3 = \gamma_c \frac{r_3^2 - r_2^2}{4 \tan \varphi_c} \quad (14)$$

The lines O_2H and O_2D are arcs r_2 and r_3 of the log-spiral. Considering the geometry of the problem

$$r_2 = \frac{H_1 \cos \theta^*}{\sin \theta_2} \quad (15)$$

$$r_3 = \frac{H_1 \cos \theta^*}{\sin \theta_2} e^{\theta_2 \tan \varphi_c} \quad (16)$$

Therefore

$$W_3 = \frac{\gamma_c H_1^2 \cos^2 \theta^*}{4 \tan \varphi_c \sin^2 \theta_2} (e^{2\theta_2 \tan \varphi_c} - 1) \quad (17)$$

The weight, W_4 , of the wedge AHO_2 is given by

$$W_4 = \frac{\gamma_c \cdot AH \cdot x_2}{2} \quad (18)$$

where

$$x_2 = \frac{-H_1 \cos \theta^* \cos(\theta^* + \theta_2)}{\sin \theta_2} \quad (19)$$

thus

$$W_4 = \frac{-\gamma_c H_1^2 \cos \theta^* \cos(\theta^* + \theta_2)}{2 \sin \theta_2} \quad (20)$$

The resultant force on plan AD of the stresses in the passive Rankine zone ADE (Fig. 4) can be written as follows (Silvestri 2003):

$$q_1 = \gamma_c AD \sin \theta^* \tan(90 - \theta^*) \quad (21)$$

The lever arms l_3 and l_4 were determined as

$$l_3 = \frac{4H_1 \xi \cos \theta^* \tan \varphi_c}{3 \sin \theta_2 (9 \tan^2 \varphi_c + 1) (e^{2\theta_2 \tan \varphi_c} - 1)} \quad (22)$$

where

$$\xi = e^{3\theta_2 \tan \varphi_c} (3 \tan \varphi_c \cos \theta^* - \sin \theta^*) + \sin(\theta^* + \theta_2) - 3 \tan \varphi_c \cos(\theta^* + \theta_2) \quad (23)$$

and

$$l_4 = \frac{-2H_1 \cos \theta^* \cos(\theta^* + \theta_2)}{3 \sin \theta_2} \quad (24)$$

Furthermore

$$y_2 = \frac{-H_1 \sin \theta^* \cos(\theta^* + \theta_2)}{\sin \theta_2} \quad (25)$$

$$AO_2 = \frac{-H_1 \cos(\theta^* + \theta_2)}{\sin \theta_2} \quad (26)$$

$$AD = \frac{H_1}{\sin \theta_2} [\cos \theta^* e^{\theta_2 \tan \varphi_c} - \cos(\theta^* + \theta_2)] \quad (27)$$

Substituting Eqs. (11), (17), and (19)–(27) into Eq. (13) gives

$$\begin{aligned} & \frac{\gamma_c \cdot H_1^3 \sin \theta^* \tan(90 - \theta^*) \cos \varphi_c}{3 \sin^3 \theta_2} [\cos \theta^* e^{\theta_2 \tan \varphi_c} - \cos(\theta^* + \theta_2)]^2 \cdot \left[\frac{1}{2} \cos(\theta^* + \theta_2) + \cos \theta^* e^{\theta_2 \tan \varphi_c} \right] + \frac{\gamma_c \cdot \xi \cdot H_1^3 \cos^3 \theta^*}{3 \sin^3 \theta_2 (9 \tan^2 \varphi_c + 1)} \\ & = \frac{\gamma_c H_1^3 \cos^2 \theta^* \cos^2(\theta^* + \theta_2)}{3 \sin^2 \theta_2} - \frac{F \cdot H_1}{2} \left\{ \frac{\sin \delta \cos \theta^* \cos(\theta^* + \theta_2)}{\sin \theta_2} - \cos \delta \left[a + \frac{\sin \theta^* \cos(\theta^* + \theta_2)}{\sin \theta_2} \right] \right\} \end{aligned} \quad (28)$$

Similar to the procedure followed for the composite-soil section, the force F is optimized with respect to θ_2 .

For the wedge (ABC) section (Fig. 5), it can be written as

$$W_w = \frac{B^2}{4} \gamma_{\text{comp}} \tan \psi \quad (29)$$

Considering the equilibrium of the soil wedge ABC gives

$$q_{\gamma u} = \frac{2P_\gamma}{B} \cos(\psi - \varphi_{\text{comp}}) - \frac{B}{4} \gamma_{\text{comp}} \tan \psi \quad (30)$$

The capacity component due to unit weight of the foundation system ($q_{\gamma u}$) is obtained by combining Eqs. (12), (28), and (30)

$$q_{\gamma u} = \frac{1}{2} \gamma_{\text{comp}} \cdot B \cdot N_\gamma \quad (31)$$

where

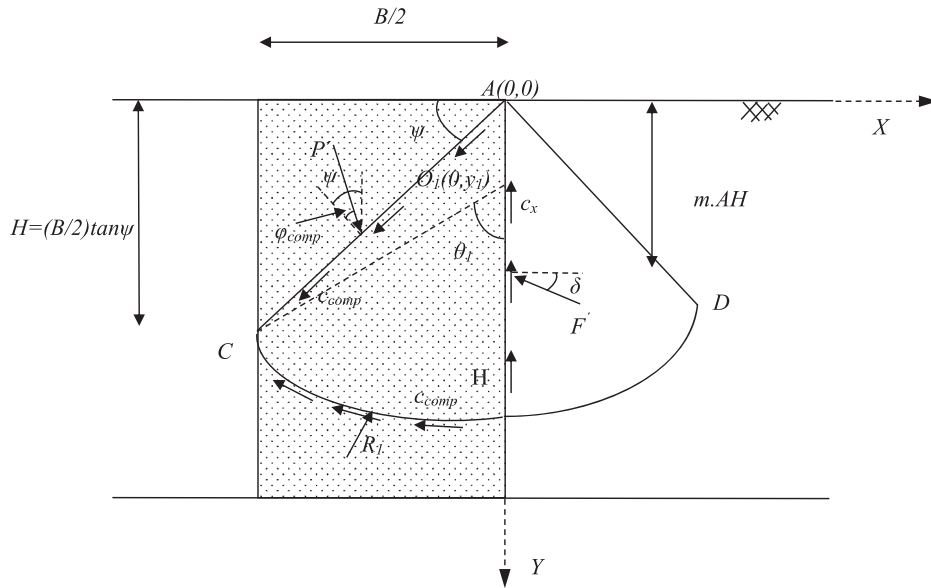


Fig. 6. External forces acting on the composite-soil section (case of: $\varphi \neq 0, \gamma = 0, q \neq 0, c \neq 0$)

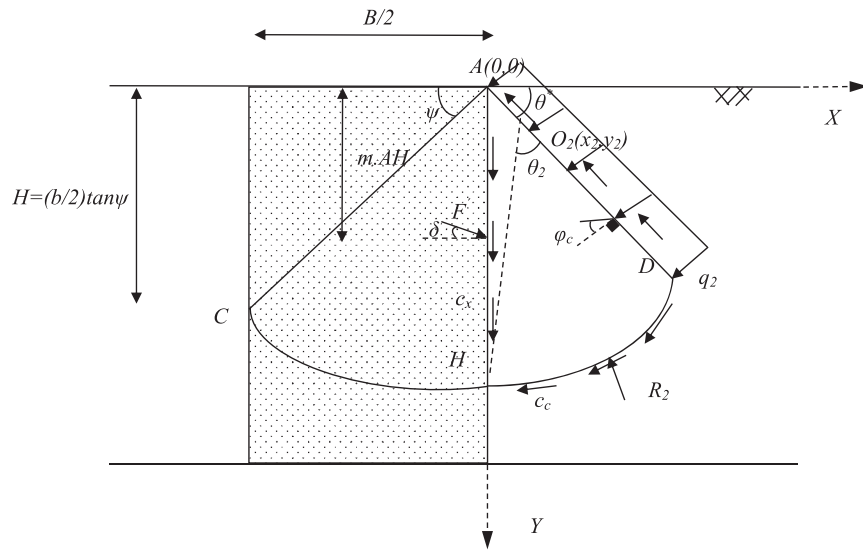


Fig. 7. External forces acting on the soft-soil section (case of: $\varphi \neq 0, \gamma = 0, q \neq 0, c \neq 0$)

$$\begin{aligned}
 & \frac{H_1^2 \cos \varphi_c \left[q \cdot \tan \left(45 + \frac{\varphi_c}{2} \right) + \frac{c_c}{\sin \left(45 - \frac{\varphi_c}{2} \right)} \right] \left[\cos^2 \theta^* e^{2\theta_2 \tan \varphi_c} - \cos^2 (\theta^* + \theta_2) \right]}{2 \sin^2 \theta_2} + \frac{c_c \cdot H_1^2 \cos^2 \theta^*}{2 \tan \varphi_c \sin^2 \theta_2} \cdot (e^{2\theta_2 \tan \varphi_c} - 1) \\
 & = H_1 \cdot F' \cdot \left\{ \cos \delta \left[m + \frac{\sin \theta^* \cos (\theta^* + \theta_2)}{\sin \theta_2} \right] - \frac{\sin \delta \cos \theta^* \cos (\theta^* + \theta_2)}{\sin \theta_2} \right\} - \frac{c_x \cdot H_1^2 \cos \theta^* \cos (\theta^* + \theta_2)}{\sin \theta_2} \quad (38)
 \end{aligned}$$

From Fig. 8, the following Eq. (39) can be derived:

$$q'_u = \frac{2P'}{B} \cos(\psi - \varphi_{comp}) + c_{comp} \tan \psi \quad (39)$$

Combining Eqs. (35), (38), and (39) and after some simplifications

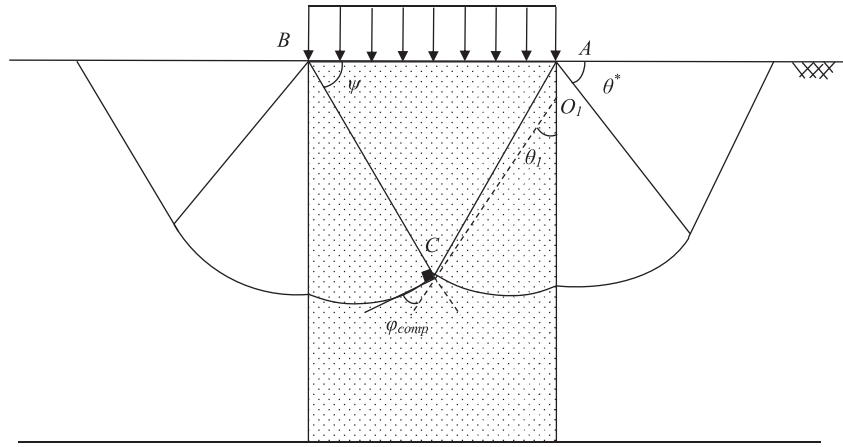


Fig. 9. Determination of the wedge angle

In this analysis, the angle θ^* was located within soil mass away from the reinforced zone; accordingly, it was taken as $45^\circ - \varphi/2$ to represent Rankine passive-pressure zone. This also was confirmed by the results of the numerical model of Hanna et al. (2013). The value of δ was taken equal to φ_c , as it is located on the slip line of the log-spiral curve in the composite soil, and c_x was taken equal to c_{comp} . Furthermore, after several iterations, the location of the force F for the cases of $q_{\gamma u}$ and q'_u was taken as $(2/3)AH$ for the case of $q_{\gamma u}$ and $(1/2)AH$ for the case of q'_u .

To estimate the minimum ultimate-bearing-capacity components ($q_{\gamma u}$ and q'_u) of the foundation system, the forces F and F' were optimized with respect to the angle θ of the log-spiral curves. The procedure was applied individually for the terms $q_{\gamma u}$ and q'_u by assuming an arbitrary value of the ultimate load per unit area, then by determining the angle of the log-spiral in the composite-soil part (θ_1) using the Newton-Raphson numerical technique [$\partial(F \text{ or } F')/\partial\theta_1 = 0$]. The angle ψ of the wedge was calculated using Eq. (45). A similar procedure was followed to determine the angle of the log-spiral curve for the soft-soil part (θ_2) by considering $\partial(F \text{ or } F')/\partial\theta_2 = 0$. The value of the term $q_{\gamma u}$ or q'_u was obtained, by trial and error, when the difference between two subsequent values of forces F or F' was equal to ± 0.01 . The mathematical calculations were coded in a computer program written in *Visual Basic 6*. The ultimate bearing capacity of the system is then given as follows:

$$q_u = q_{\gamma u} + q'_u \quad (46)$$

The produced bearing-capacity factors (N_γ , N_q , and N_c) in this investigation were grouped and presented in the form of design charts in Figs. 10–12 for $\gamma_{\text{comp}}/\gamma_c$ from 1 to 2 and for c_{comp}/c_c from 0.2 to 0.8, which were believed to cover a wide range of practical cases. Furthermore, linear interpolation may be used for intermediate values. The pronounced effect of native soil strength on the bearing capacity of the ground can be seen in these figures. Notably, owing to the increase of the unit weight of the reinforced area, the driving force of the system increases and the bearing capacity decreases. Furthermore, an increase in the strength of the native soil increases the resistant force against the foundation load and, accordingly, increases the bearing capacity of the system.

Thus

$$q_u = \frac{1}{2} \gamma_{\text{comp}} B N_\gamma + q N_q + c_{\text{comp}} N_c \quad (47)$$

where c_{comp} , γ_{comp} , and φ_{comp} are the cohesion, unit weight, and angle of shearing resistance of the equivalent soil/column system (composite system) and are given as follows:

$$c_{\text{comp}} = A_s c_s + (1 - A_s) c_c \quad (48)$$

$$\gamma_{\text{comp}} = A_s \gamma_s + (1 - A_s) \gamma_c \quad (49)$$

and

A_s = replacement ratio

$$(A_s = A_{\text{col}}/s^2 \text{ for a square-column pattern}) \quad (50)$$

where A_{col} and s = cross section of the column and the spacing between columns, respectively; and c_s and c_c = cohesions of column's material (stone) and soil (clay), respectively. In this analysis, the cohesion for the stone material (c_s) was assumed to be zero; and γ_s and γ_c = unit weights of column and soil materials, respectively.

Mohr-Coulomb failure criterion for the composite system is represented as

$$\tau_{\text{comp}} = A_s \tau_s + (1 - A_s) \tau_c \quad (51)$$

Consequently, the angle of shearing resistance of the composite system can be given by

$$\varphi_{\text{comp}} = \tan^{-1} [A_s \mu_s \tan \varphi_s + (1 - A_s) \mu_c \tan \varphi_c] \quad (52)$$

where

$$\mu_s = \frac{n}{1 + (n - 1)A_s} \quad (53)$$

$$\mu_c = \frac{1}{1 + (n - 1)A_s} \quad (54)$$

τ_{comp} , τ_s , and τ_c = shear strength of the composite soil, stone column, and the soft soil, respectively; φ_s and φ_c = angle of shearing resistance of the material of the stone column and the soft soil, respectively; and n = stress ratio, which is defined as the ratio between vertical stress in the granular material and the cohesive soil.

Mitchell and Katti (1981) suggested that n is in the range of 2 to 6 and usually has the value of 3 to 4 for stone columns in clay, which is in agreement with the range of 2 to 5 reported by Barksdale and Bachus (1983) and the range of 2 to 4 reported by Fattah et al. (2011). McKelvey et al. (2004) reported that, at higher loadings, the value of

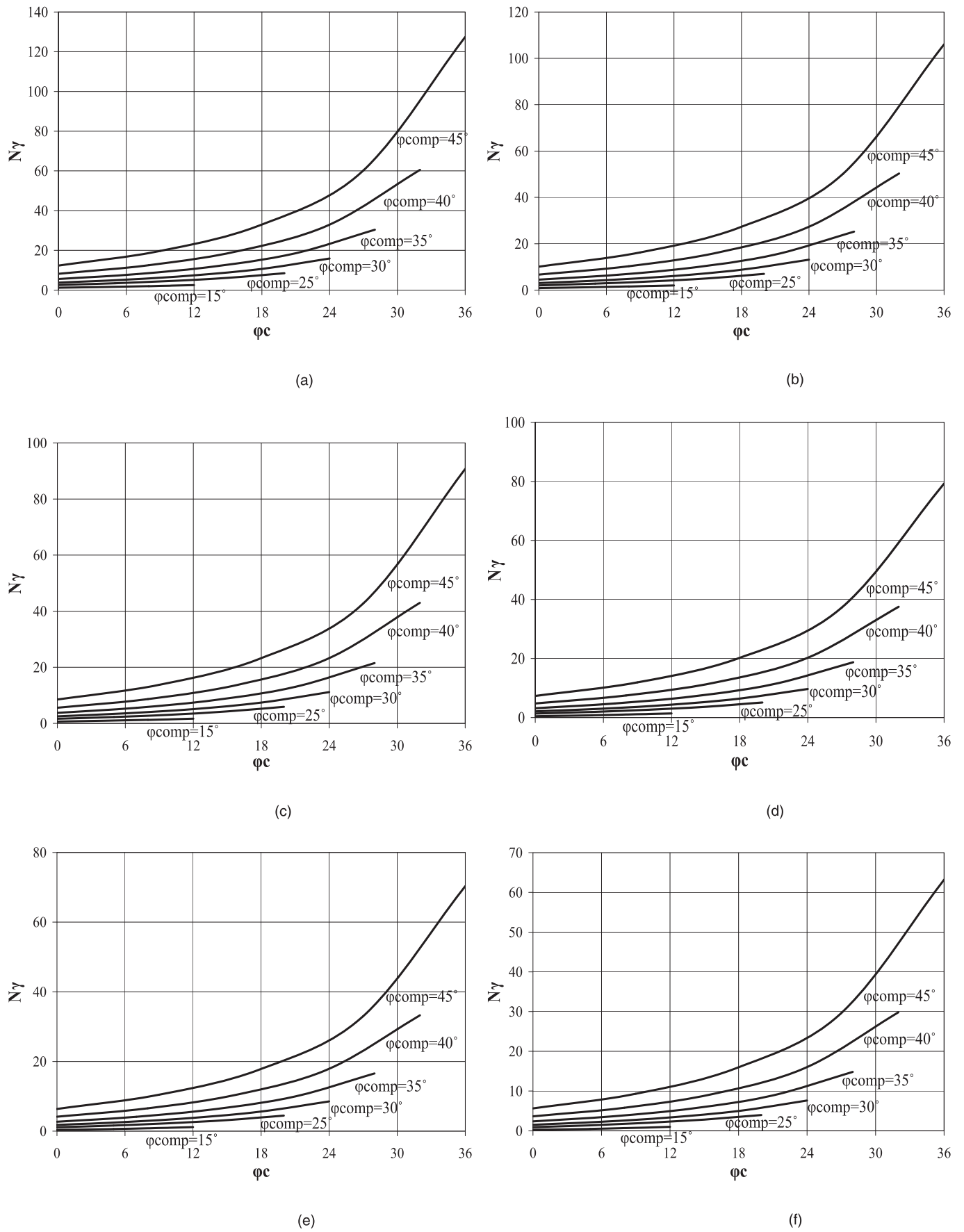


Fig. 10. N_γ versus angles of shearing resistance for the reinforced ground: (a) $\gamma_{comp}/\gamma_c = 1$; (b) $\gamma_{comp}/\gamma_c = 1.2$; (c) $\gamma_{comp}/\gamma_c = 1.4$; (d) $\gamma_{comp}/\gamma_c = 1.6$; (e) $\gamma_{comp}/\gamma_c = 1.8$; (f) $\gamma_{comp}/\gamma_c = 2$

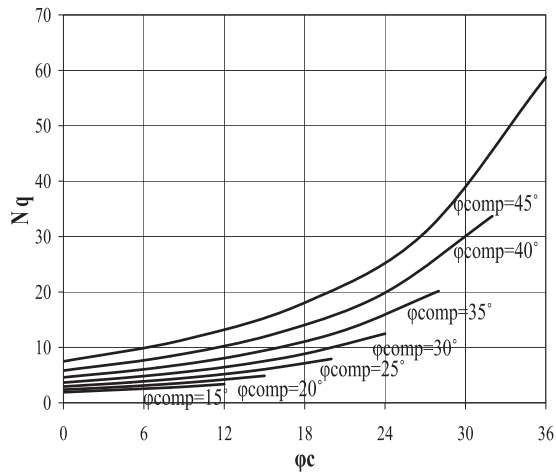


Fig. 11. N_q versus angles of shearing resistance for the reinforced ground

n approaches 3. Han and Ye (2002) reported that the stress-concentration ratio is equal to the ratio of the volumetric compressibility coefficient of the soil to that of the stone columns; whereas, based on finite-element study, Ambily and Gandhi (2007) presented a figure showing that the stress-concentration ratio can be estimated based on the ratio of column spacing/column diameter, undrained shear strength of soft soil, and the modulus of elasticity ratio of stone columns to the soft soil.

Enoki et al. (1991) proposed another equivalent soil model, which considers the anisotropy for the ground reinforced with stone columns. Accordingly, those authors derived the following equations:

$$\varphi_{\text{comp}} = \frac{\pi}{2} - 2 \tan^{-1} \sqrt{K_a} \quad (55)$$

$$c_{\text{comp}} = (1 - A_s)c_c \sqrt{K_a} \quad (56)$$

where

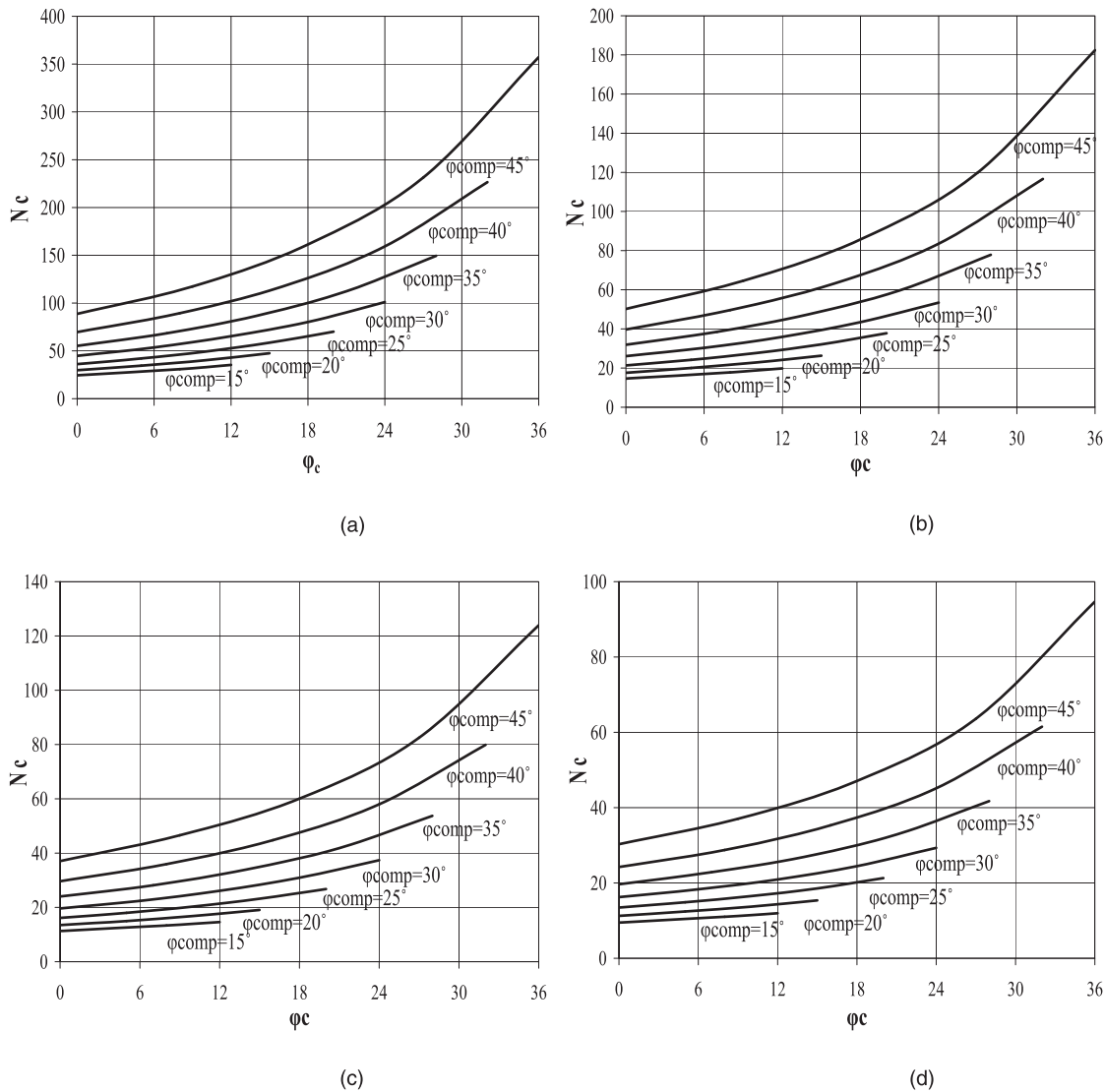


Fig. 12. N_c versus angles of shearing resistance for the reinforced ground: (a) $c_{\text{comp}}/c_c = 0.2$; (b) $c_{\text{comp}}/c_c = 0.4$; (c) $c_{\text{comp}}/c_c = 0.6$; (d) $c_{\text{comp}}/c_c = 0.8$

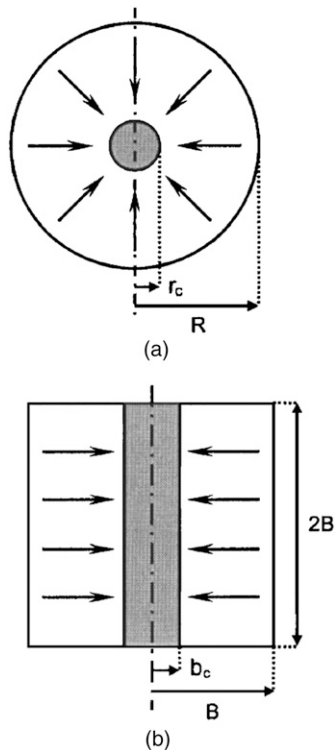


Fig. 13. Conversion of stone columns from (a) 3D to (b) plane strain (Reprinted from Tan et al. 2008, © ASCE)

$$K_a = \frac{1 - \sin \varphi_s}{1 + (2A_s - 1)\sin \varphi_s} \quad (57)$$

The method proposed by Tan et al. (2008) was used to convert the plane-strain condition used in this model to the real three-dimensional (3D) condition where the width of the stone columns is adjusted to Br_c^2/R^2 , where r_c , R , and B are column and cell radius in the actual case and equivalent plane-strain width, respectively (Fig. 13). For square-pattern columns, $R = 1.13B$. The plane-strain model was used previously to model the group of stone column—reinforced ground by Madhav and Vitkar (1978), Priebe (1995), and Deb et al. (2007), without any 3D conversion.

The concept of replacing a soil/column system with an equivalent soil was used before by researchers such as Barksdale and Bachus (1983), Priebe (1995), Bouassida et al. (1995), Lee and Pande (1998), and Hassen et al. (2010, 2013).

Column-Installation Effect

During the construction of stone columns, it is expected that soil adjacent to the columns undergoes some disturbances and smear effect, which may influence the performance of the stone columns. Weber et al. (2010) divided the disturbed area into three zones: (1) penetration zone, where the sand particles are squeezed into the clay; (2) smear zone, where soil particles experience significant reorientation; and (3) densification zone, where the structure of the clay does not appear to change but compaction of the clay is measurable.

Table 1. Comparison of N_γ between the Results Obtained by the Present Theory and the Classic Theories for Homogeneous Soils

Angle φ (degrees)	Bearing capacity factor (N_γ)						Angle ψ (degrees)		
	Present study	Vesic (1973)	Chen (1975)	Terzaghi (1943)	Soubra (1999)	Frydman and Burd (1997)	Bouassida and Jellali (2002)	Present study	$45 + \varphi/2$
15	2.90	2.65	2.94	1.52	1.95			51.6	52.5
16	3.39	3.06	3.42	1.82	2.32		3.82	51.7	53.0
17	3.94	3.53	3.98	2.18	2.75			51.8	53.5
18	4.51	4.07	4.61	2.59	3.25			52.0	54.0
19	5.17	4.68	5.35	3.07	3.82			52.3	54.5
20	5.95	5.39	6.20	3.64	4.49			52.6	55.0
21	6.82	6.20	7.18	4.31	5.26			52.9	55.5
22	7.83	7.13	8.32	5.09	6.15			53.3	56.0
23	9.00	8.20	9.64	6.00	7.19			53.7	56.5
24	10.37	9.44	11.18	7.08	8.40			54.1	57.0
25	11.95	10.88	12.97	8.34	9.81			54.6	57.5
26	13.78	12.54	15.05	9.84	11.46		16.61	55.0	58.0
27	15.92	14.47	17.50	11.60	13.39			55.5	58.5
28	18.43	16.72	20.36	13.70	15.67			56.0	59.0
29	21.37	19.34	23.72	16.18	18.35			56.5	59.5
30	24.85	22.40	27.67	19.13	21.51	21.70		57.0	60.0
31	28.91	25.99	32.34	22.65	25.26			57.5	60.5
32	33.76	30.22	37.86	26.87	29.71			58.0	61.0
33	39.47	35.19	44.41	31.94	35.02			58.6	61.5
34	36.33	41.06	52.20	38.04	41.37			59.1	62.0
35	54.49	48.03	61.49	45.41	49.00	54.20		59.6	62.5
36	64.33	56.31	72.62	54.36	58.21			60.7	63.0
37	76.22	66.19	85.98	65.27	69.35			60.7	63.5
38	90.61	78.03	102.10	78.61	82.91		113.61	61.3	64.0
39	108.15	92.25	121.60	95.03	99.48			61.8	64.5
40	129.63	109.41	145.30	115.31	119.84	147.00	163.5	62.1	65.0

Table 2. Comparison of N_q between the Results Obtained by the Present Theory and the Classic Theories for Homogeneous Soils

Angle φ (degrees)	Bearing capacity factor (N_q)						Angle ψ (degrees)		
	Present study	Vesic (1973)	Terzaghi (1943)	Silvestri (2003)	Soubra (1999)	Chen (1975)	Bouassida and Jellali (2002)	Present study	$45 + \varphi/2$
15	3.96	3.94	4.45		3.95	3.94		52.5	52.5
16	4.33	4.34	4.92		4.34	4.34	4.33	53.0	53.0
17	4.79	4.77	5.45		4.78	4.77		53.5	53.5
18	5.27	5.26	6.04		5.27	5.26		54.0	54.0
19	5.79	5.80	6.70		5.81	5.80		54.5	54.5
20	6.39	6.40	7.44		6.41	6.40		55.0	55.0
21	7.06	7.07	8.26		7.08	7.07		55.5	55.5
22	7.82	7.82	9.19		7.84	7.82		56.0	56.0
23	8.65	8.66	10.23		8.68	8.66		56.5	56.5
24	9.59	9.60	11.40		9.62	9.61		57.0	57.0
25	10.64	10.66	12.72	10.91	10.69	10.66		57.5	57.5
26	11.87	11.85	14.21	12.14	11.88	11.86	11.85	58.0	58.0
27	13.19	13.20	15.90	13.36	13.23	13.20		58.5	58.5
28	14.72	14.72	17.81	15.10	14.76	14.72		59.0	59.0
29	16.44	16.44	19.98	16.87	16.49	16.45		59.5	59.5
30	18.40	18.40	22.46	18.89	18.46	18.41		60.0	60.0
31	20.63	20.63	25.28	21.20	20.70	20.64		60.5	60.5
32	23.18	23.18	28.52	23.83	23.26	23.18		61.0	61.0
33	26.06	26.09	32.23	26.84	26.19	26.10		61.4	61.5
34	29.44	29.44	36.50	30.30	29.56	29.45		62.0	62.0
35	33.27	33.30	41.44	34.29	33.44	33.31		62.5	62.5
36	37.75	37.75	47.16	38.91	37.93	37.76		63.0	63.0
37	42.95	42.92	53.80	44.25	43.13	42.93		63.5	63.5
38	48.93	48.93	61.55	50.49	49.19	48.95	48.93	64.0	64.0
39	55.95	55.96	70.61	57.77	56.28	55.97		64.5	64.5
40	64.19	64.20	81.27	66.31	64.58	64.21	64.19	65.0	65.0

Table 3. Comparison of N_c between the Results Obtained by the Present Theory and the Classic Theories for Homogeneous Soils

Angle φ (degrees)	Bearing capacity factor (N_c)						Angle ψ (degrees)	
	Present study	Vesic (1973)	Terzaghi (1943)	Soubra (1999)	Chen (1975)	Bouassida and Jellali (2002)	Present study	$45 + \varphi/2$
15	10.96	10.98	12.86	10.99	10.98		52.5	52.5
16	11.62	11.63	13.68	11.65	11.63	11.63	53.0	53.0
17	12.34	12.34	14.60	12.36	12.34		53.5	53.5
18	13.08	13.10	15.12	13.13	13.11		54.0	54.0
19	13.92	13.93	16.57	13.96	13.94		54.5	54.5
20	14.82	14.83	17.69	14.86	14.84		55.0	55.0
21	15.79	15.82	18.92	15.85	15.82		55.5	55.5
22	16.88	16.88	20.27	16.92	16.89		56.0	56.0
23	18.02	18.05	21.75	18.09	18.05		56.5	56.5
24	19.30	19.32	23.36	19.37	19.33		57.0	57.0
25	20.71	20.72	25.13	20.77	20.73		57.5	57.5
26	22.24	22.25	27.09	22.32	22.26	22.25	58.0	58.0
27	23.93	23.94	29.24	24.01	23.95		58.5	58.5
28	25.80	25.80	31.61	25.88	25.81		59.0	59.0
29	27.86	27.86	34.24	27.95	27.87		59.5	59.5
30	30.11	30.14	37.16	30.24	30.15		60.0	60.0
31	32.67	32.67	40.41	32.79	32.68		60.5	60.5
32	35.46	35.49	44.04	35.62	35.50		61.0	61.0
33	38.60	38.64	48.09	38.79	38.65		61.4	61.5
34	46.13	42.16	52.64	42.34	42.18		62.0	62.0
35	46.12	46.12	57.75	46.33	46.14		62.5	62.5
36	50.55	50.59	63.53	50.82	50.50		63.0	63.0
37	55.69	55.63	70.01	55.91	55.65		63.5	63.5
38	61.36	61.35	77.50	61.68	61.37	61.35	64.0	64.0
39	67.87	67.87	85.97	68.25	67.89		64.5	64.5
40	75.31	75.31	95.66	75.77	75.34	75.31	65.0	65.0

Table 4. Comparison between the Ultimate Bearing Capacities of Ground Reinforced with a Group of Stone Columns Predicted by the Present Theory and Available Experimental Results and Numerical Data

Number	c_u or c (kPa)	φ_s (degrees)	φ_c (degrees)	γ_c ($\text{kN} \cdot \text{m}^3$)	γ_s ($\text{kN} \cdot \text{m}^3$)	A_s (%)	B (m)	q (kPa)	q_u Measured (kPa)	q_u Present theory (kPa)
1 ^a	32	34	0	14	17.3	24	0.09	0	272	265
2 ^a	20.5	34	0	9.9	20.3	40	0.05	0	160	176
3 ^b	10.5	30	0	13.1	15.47	30	0.1	0	79	85
4 ^b	11.5	30	0	13.1	15.47	30	0.1	0	75	93
5 ^c	5	45	25	16.0	21	35	2.5	3.2	800	870
6 ^c	5	45	12	13.0	21	35	2.5	2.6	352	334
7 ^c	5	40	13	13.0	19	35	2.5	2.6	280	293
8 ^c	5	45	15	14.0	21	35	2.5	2.8	420	392
9 ^c	15	45	15	14.0	21	35	2.5	2.8	660	618
10 ^c	5	40	13	13.0	19	30	2.62	2.6	275	261
11 ^c	10	40	13	13.0	19	30	2.62	2.6	366	347
12 ^c	15	40	13	13.0	19	30	2.62	2.6	458	433
13 ^c	5	45	12	12.0	21	35	3	2.6	365	350
14 ^c	12	45	12	12.0	21	35	3	2.6	508	491

^aData from experimental work of McKelvey et al. (2004).

^bData from experimental work of Hu (1995).

^cData from numerical study of Hanna et al. (2013).

Elshazly et al. (2008) reported the average of postinstallation horizontal to vertical stress ratio, K , of 1.2 based on numerical modeling and validation with the experimental work, which is close to the value of 1 proposed by Priebe (1995). Egan et al. (2009) reported that, at this time, it does not appear to be an acceptable, rigorous means to account for the column-installation effect. Weber et al. (2010) recommended the need to study the effect of the remolded zone on possible reduction in bearing capacity of the stone/soil system. Utilizing finite-element technique, Castro and Karstunen (2010) suggested a rough 15–20% reduction of the undrained shear strength of the soil owing to the column-installation effect. McCabe et al. (2009) reported two studies, the first of which suggested an increase in horizontal stress whereas the second of which stated the disappearance of the increase in the horizontal stress in the soil once the installation of the stone columns was complete. Six et al. (2012) recommended increasing the efficiency of the stone columns by increasing the value of K as a result of the installation effect; the decrease of the clay undrained strength owing to the smear effect, however, was not discussed in the paper. Indraratna et al. (2013) reported that the effect of clogging influences the pattern of settlement at the initial stage of consolidation.

In this study, Castro and Karstunen's (2010) recommendation was adopted in developing the present theory.

Validation

The theory presented in this paper was validated first with the classic theories for shallow foundation on homogenous soil. In this case, the cohesion and the angle of shearing resistance of the composite soil and the soft soil were replaced by the values for the homogenous soil. The values of N_γ , N_q , and N_c were calculated for different values of φ (Tables 1–3). Notably, good agreements between the predicted and values for the bearing-capacity factors N_c and N_q were found. Furthermore, the proposed value for the wedge angle [Eq. (45)] was in good agreement with the angle $45^\circ + \varphi/2$, which was proposed in the classic theories for homogeneous soils by several researchers. For the case of N_γ , the values predicted by the proposed theory were slightly higher than those of Vesic (1973) and Soubra (1999) and

lower than those of Chen (1975) and Bouassida and Jellali (2002). Although these discrepancies are within the acceptable range in the field of geotechnical engineering, they may be attributed to the difference in the values assumed for the wedge angle ψ .

Furthermore, the ultimate bearing capacity predicted by the proposed theory [Eq. (47)] was compared with laboratory test results and the numerical data available in the literature for the case of a group of stone columns installed in soft soil. The results of this comparison are presented in Table 4, where good agreement is apparent.

Conclusion

An analytical model was developed for the case of a group of stone columns in soft soil subjected to general shear failure. The model is capable of predicting the ultimate bearing capacity of the reinforced ground. The following may be concluded from this study:

1. The limit-equilibrium technique is a viable method of analysis to model the case of soft soil reinforced with stone columns.
2. The failure mechanism of the stone columns and the surrounding soil was successfully idealized by a wedge, two log-spiral curves, and a passive Rankine section.
3. The bearing capacity of the system can be determined by using the general bearing-capacity equation of Terzaghi (1943) and the bearing-capacity factors N_γ , N_q , and N_c given in this paper.
4. The results produced by the present theoretical model compared well with the theories available for homogenous soil.
5. The results produced by the present theoretical model compared well with the experimental and numerical results available in the literature for reinforced earth.
6. Design charts are presented for the prediction of the bearing-capacity factors N_γ , N_q , and N_c for the case of reinforced soil.

Acknowledgments

The financial support from the Natural Science and Engineering Research Council of Canada and Concordia University are gratefully acknowledged.

References

- Ambily, A. P., and Gandhi, S. R. (2007). "Behavior of stone columns based on experimental and FEM analysis." *J. Geotech. Geoenviron. Eng.*, 10.1061/(ASCE)1090-0241(2007)133:4(405), 405–415.
- Asgari, A., Olliaei, M., and Bagheri, M. (2013). "Numerical simulation of improvement of a liquefiable soil layer using stone column and pile-pinning techniques." *Soil. Dyn. Earthquake Eng.*, 51(Aug.), 77–96.
- Balaam, N. P., and Booker, J. R. (1981). "Analysis of rigid rafts supported by granular piles." *Int. J. Numer. Anal. Methods Geomech.*, 5(4), 379–403.
- Barksdale, R. D., and Bachus, R. C. (1983). "Design and construction of stone columns: Volume 1." *Rep. No. FHWA/RD-83/026*, Federal Highway Administration, Washington, DC.
- Bouassida, M., de Buhan, P., and Dormieux, L. (1995). "Bearing capacity of a foundation resting on a soil reinforced by a group of columns." *Geotechnique*, 45(1), 25–34.
- Bouassida, M., and Jellali, B. (2002). "Capacité portante d'un sol renforcé par une tranchée." *Revue Française de Génie Civil*, 6(7–8), 1381–1395 (in French).
- Bouassida, M., Jellali, B., and Porbaha, A. (2009). "Limit analysis of rigid foundations on floating columns." *Int. J. Geomech.*, 10.1061/(ASCE)1532-3641(2009)9:3(89), 89–101.
- Castro, J., and Karstunen, M. (2010). "Numerical simulations of stone column installation." *Can. Geotech. J.*, 47(10), 1127–1138.
- Chen, W. F. (1975). *Limit analysis and soil plasticity*, Elsevier, New York.
- Deb, K., Basudhar, P. K., and Chandra, S. (2007). "Generalized model for geosynthetic-reinforced granular fill-soft soil with stone columns." *Int. J. Geomech.*, 10.1061/(ASCE)1532-3641(2007)7:4(266), 266–276.
- Egan, D., Scott, W., and McCabe, B. (2009). "Installation effects of vibro replacement stone columns in soft clay." *Geotechnics of soft soils: Focus on ground improvement*, M. Karstunen and M. Leoni, eds., CRC Press/Balkema, London, 23–29.
- Ellouze, S., Bouassida, M., Hazzar, L., and Mroueh, H. (2010). "On settlement of stone column foundation by Priebe's method." *Proc. Inst. Civ. Eng. Ground Improv.*, 163(2), 101–107.
- Elshazly, H., Elkasabgy, M., and Elleboudy, A. (2008). "Effect of inter-column spacing on soil stresses due to vibro-installed stone columns: Interesting findings." *Geotech. Geol. Eng.*, 26(2), 225–236.
- Enoki, M., Yagi, N., Yatabe, R., and Ichimoto, E. (1991). "Shearing characteristic of composite ground and its application to stability analysis." *Deep foundation improvements: Design, construction, and testing*, M. I. Esrig and R. C. Bachus, eds., ASTM, West Conshohocken, PA, 19–31.
- Fattah, M. Y., Shlash, K. T., and Al-Waily, M. J. M. (2011). "Stress concentration ratio of model stone columns in soft clays." *ASTM Geotech. Test. J.*, 34(1), 1–11.
- Frydman, S., and Burd, H. J. (1997). "Numerical studies of bearing-capacity factor N_{γ} ." *J. Geotech. Geoenviron. Eng.*, 10.1061/(ASCE)1090-0241(1997)123:1(20), 20–29.
- Han, J., and Ye, S. L. (2002). "A theoretical solution for consolidation rates of stone column-reinforced foundations accounting for smear and well resistance effects." *Int. J. Geomech.*, 10.1061/(ASCE)1532-3641(2002)2:2(135), 135–151.
- Hanna, A. M., Etezad, M., and Ayadat, T. (2013). "Mode of failure of a group of stone columns in soft soil." *Int. J. Geomech.*, 10.1061/(ASCE)GM.1943-5622.0000175, 87–96.
- Hassen, G., de Buhan, P., and Abdelkrim, M. (2010). "Finite element implementation of a homogenized constitutive law for stone column-reinforced foundation soils, with application to the design of structures." *Comput. Geotech.*, 37(1–2), 40–49.
- Hassen, G., Gueguin, M., and de Buhan, P. (2013). "A homogenization approach for assessing the yield strength properties of stone column reinforced soils." *Eur. J. Mech. A, Solids*, 37(Jan.–Feb.), 266–280.
- Hijab, W. A. (1956). "A note on the centroid of a logarithmic spiral sector." *Geotechnique*, 6(2), 66–69.
- Hu, W. (1995). "Physical modeling of group behavior of stone column foundations." Ph.D. dissertation, Univ. of Glasgow, Glasgow, U.K.
- Hu, W., Wood, D. M., and Stewart, W. (1997). "Ground improvement using stone column foundations: Result of model tests." *Proc., Int. Conf. on Ground Improvement Technology*, CI-Premier, Singapore, 247–256.
- Hughes, J. M. O., and Withers, N. J. (1974). "Reinforcing of soft cohesive soils with stone columns." *Ground Eng.*, 7(3), 42–49.
- Indraratna, B., Basack, S., and Rujikiatkamjorn, C. (2013). "Numerical solution of stone column-improved soft soil considering arching, clogging, and smear effects." *J. Geotech. Geoenviron. Eng.*, 10.1061/(ASCE)GT.1943-5606.0000789, 377–394.
- Kaliakin, V. N., Khabbaziyan, M., and Meehan, C. L. (2012). "Modeling the behavior of geosynthetic encased columns: Influence of granular soil constitutive model." *Int. J. Geomech.*, 10.1061/(ASCE)GM.1943-5622.0000084, 357–369.
- Kumbhojkar, A. S. (1993). "Numerical evaluation of Terzaghi's N_{γ} ." *J. Geotech. Geoenviron. Eng.*, 10.1061/(ASCE)0733-9410(1993)119:3(598), 598–607.
- Lee, J. S., and Pande, G. N. (1998). "Analysis of stone-column reinforced foundations." *Int. J. Numer. Anal. Methods Geomech.*, 22(12), 1001–1020.
- Madhav, M. R., and Vitkar, P. P. (1978). "Strip footing on weak clay stabilized with a granular trench or pile." *Can. Geotech. J.*, 15(4), 605–609.
- McCabe, B. A., Nimmons, G. J., and Egan, D. (2009). "A review of field performance of stone columns in soft soils." *Proc. Inst. Civ. Eng. Geotech. Eng.*, 162(6), 323–334.
- McKelvey, D., Sivakumar, V., Bell, A., and Graham, J. (2004). "Modelling vibrated stone columns in soft clay." *Proc. Inst. Civ. Eng. Geotech. Eng.*, 157(3), 137–149.
- Mitchell, J. K., and Katti, R. K. (1981). "Soil improvement state-of-the-art report." *Proc., 10th Int. Conf. on Soil Mechanics and Foundation Engineering*, Vol. 4, Balkema, Rotterdam, Netherlands, 509–565.
- Mokhtari, M., and Kalantari, B. (2012). "Soft soil stabilization using stone columns—A review." *Electronic J. Geotech. Eng.*, 17, 1659–1666.
- Muir Wood, D., Hu, W., and Nash, D. F. T. (2000). "Group effects in stone column foundations: Model tests." *Geotechnique*, 50(6), 689–698.
- Najjar, S. S. (2013). "A state-of-the-art review of stone/sand-column reinforced clay systems." *Geotech. Geol. Eng.*, 31(2), 355–386.
- Priebe, H. J. (1995). "The design of vibro replacement." *Ground Eng.*, 28(10), 31–37.
- Priebe, H. J. (2005). "Design of vibro replacement." *Ground Eng.*, 38(1), 25–27.
- Shahu, J. T., and Reddy, Y. R. (2011). "Clayey soil reinforced with stone column group: Model tests and analyses." *J. Geotech. Geoenviron. Eng.*, 10.1061/(ASCE)GT.1943-5606.0000552, 1265–1274.
- Silvestri, V. (2003). "A limit equilibrium solution for bearing capacity of strip foundations on sand." *Can. Geotech. J.*, 40(2), 351–361.
- Six, V., Mroueh, H., Shahrou, I., and Bouassida, M. (2012). "Numerical analysis of elastoplastic behavior of stone column foundation." *Geotech. Geol. Eng.*, 30(4), 813–825.
- Soubra, A.-H. (1999). "Upper-bound solutions for bearing capacity of foundations." *J. Geotech. Geoenviron. Eng.*, 10.1061/(ASCE)1090-0241(1999)125:1(59), 59–68.
- Stuedlein, A. W., and Holtz, R. D. (2013). "Bearing capacity of spread footings on aggregate pier reinforced clay." *J. Geotech. Geoenviron. Eng.*, 10.1061/(ASCE)GT.1943-5606.0000748, 49–58.
- Stuedlein, A. W., and Holtz, R. D. (2014). "Displacement of spread footings on aggregate pier reinforced clay." *J. Geotech. Geoenviron. Eng.*, 10.1061/(ASCE)GT.1943-5606.0000982, 36–45.
- Tan, S. A., Tjahjono, S., and Oo, K. K. (2008). "Simplified plane-strain modeling of stone-column reinforced ground." *J. Geotech. Geoenviron. Eng.*, 10.1061/(ASCE)1090-0241(2008)134:2(185), 185–194.
- Terzaghi, K. (1943). *Theoretical soil mechanics*, Wiley, New York.
- Vesic, A. S. (1973). "Analysis of ultimate loads of shallow foundations." *J. Soil Mech. and Found. Div.*, 99(1), 45–73.
- Visual Basic 6* [Computer software]. Redmond, WA, Microsoft.
- Weber, T. M., Plotze, M., Laue, J., Peschke, G., and Springman, S. M. (2010). "Smear zone identification and soil properties around stone columns constructed in-flight in centrifuge model tests." *Geotechnique*, 60(3), 197–206.
- Wehr, W. (1999). "Schottersäulen – das Verhalten von einzelnen Säulen und Säulengruppen." *Geotechnik*, 22(1), 40–47 (in German).